Interaction of a Peptide Derived from Glycoprotein gp36 of Feline Immunodeficiency Virus and Its Lipoylated Analogue with Phospholipid Membranes

Gerardino D'Errico,[‡] Anna Maria D'Ursi,[§] and Derek Marsh*[,||]

Dipartimento di Chimica, Università di Napoli "Federico II", Napoli, Italy, Dipartimento di Scienze Farmaceutiche, Università di Salerno, Fisciano, Italy, and Max-Planck-Institut für biophysikalische Chemie, Abt. Spektroskopie, Göttingen, Germany

Received December 21, 2007; Revised Manuscript Received March 6, 2008

ABSTRACT: P59, a 20-mer peptide modeled on the membrane-proximal external region (MPER) of the feline immunodeficiency virus (FIV) gp36 ectodomain, has potent antiviral activity. The lipoylated analogue, lipo-P59, displays a similar activity, which is preferentially retained by cellular substrates. A mechanism has been proposed recently in which the peptide, being positioned on the surface of the cell membrane, inhibits its fusion with the virus; the lipophilic chain of lipo-P59 is thought to insert into the membrane interior, thus anchoring the peptide at the surface. In the present work, lipid−peptide interactions of P59 and lipo-P59 with phospholipid liposomes are investigated using spin-label electron spin resonance spectroscopy. Two phospholipids have been examined, the zwitterionic dimyristoyl phosphatidylcholine and the anionic dimyristoyl phosphatidylglycerol, and a wide range of lipid spin labels, including positional isomers. Independent of the membrane charge, both peptides bind to lipid bilayers; however, whereas P59 insertion between the lipid headgroups leads to significant liposome destabilization, eventually resulting in vesicle fragmentation with the formation of smaller aggregates, lipo-P59 inserts with the lipophilic tail among the lipid chains, while the peptidic portion remains adsorbed onto the membrane, where it can effectively exert its antiviral activity.

Fusion of the phospholipid membrane enveloping a virus with that of the target cell is a fundamental step in viral infection (*1*). The energetic barrier that hinders spontaneous fusion between the two apposing membranes is overcome by specific transmembrane proteins present in the viral envelope. Fusion proteins from distantly related viruses lack apparent sequence homology. Nevertheless, most share a common functional mechanism, in which a hydrophobic domain (the so-called "fusion peptide") inserts in the target cell membrane, generating an intermediate that is anchored to both the cellular and viral membranes. Subsequent folding of the protein brings the membranes in close proximity, thus favoring their fusion. However, there is converging evidence that protein domains other than the fusion peptide play an important role in the membrane fusion.

Similar to the human immunodeficiency virus (HIV),[1] the feline immunodeficiency virus (FIV) (*2, 3*) effects cell entry via a molecular mechanism that involves such a surface glycoprotein (*4*−*6*). Despite the low sequence homology, the FIV and HIV glycoproteins, named gp36 and gp41, respectively, possess a common structural architecture consisting of a transmembrane (TM) region and membrane-proximal segment (pre-TM) that is directly involved in the virus−target cell fusion. Furthermore, both proteins contain an unusual clustering of tryptophan residues in the membrane-proximal external region (MPER) of the ectodomain of the TM region (*7*−*9*). Peptides deriving from MPER of gp41 are able to prevent HIV−cell membrane fusion (*10*−*12*), and one of these, formerly known as peptide T-20, is used clinically as an anti-HIV fusion inhibitor (*13*). In the same way, peptides derived from MPER of gp36 display anti-FIV activity (*14, 15*).

MPER-derived peptides are assumed to exert antiviral activity by adsorbing on the external surface of the target-

* To whom correspondence should be addressed: Max-Planck-Institut für biophysikalische Chemie, Abt. Spektroskopie, Göttingen, Germany. Telephone: +49-551-2011285. Fax: +49-551-2011501. E-mail: dmarsh@gwdg.de.

[‡] Università di Napoli "Federico II".

[§] Università di Salerno.

[||] Max-Planck-Institut für biophysikalische Chemie.

[1] Abbreviations: 5-PASL, 1-acyl-2-[5-(4,4-dimethyloxazolidine-*N*-oxyl)]stearoyl-*sn*-glycero-3-phosphatidic acid; 5-PESL, 1-acyl-2-[5-(4,4-dimethyloxazolidine-*N*-oxyl)]stearoyl-*sn*-glycero-3-phosphoethanolamine; 5-PSSL, 1-acyl-2-[5-(4,4-dimethyloxazolidine-*N*-oxyl)]stearoyl-*sn*-glycero-3-phosphoserine; Aod, 2-aminooctadecanoic acid; CD, circular dichroism; DMPC, dimyristoyl phosphatidylcholine; DMPG, dimyristoyl phosphatidylglycerol; DPC, dodecylphosphocholine; EDTA, ethylenediaminetetraacetic acid; ESR, electron spin resonance; FIV, feline immunodeficiency virus; HBS, Hepes-buffered saline buffer; HEPES, *N*-(2-hydroxyethyl)piperazine-*N*′-2-ethanesulfonic acid; HIV, human immunodeficiency virus; lipo-P59, analogue of P59 lipoylated at the C terminus; MPER, membrane-proximal external region of the viral glycoprotein; MPEx, Membrane Protein Explorer package; *n*-PCSL, 1-acyl-2-[*n*-(4,4-dimethyloxazolidine-*N*-oxyl)]stearoyl-*sn*-glycero-3-phosphocholine; *n*-PGSL, 1-acyl-2-[*n*-(4,4-dimethyloxazolidine-*N*-oxyl)]stearoyl-*sn*-glycero-3-phosphoglycerol; P59, 20-mer peptide modeled on the membrane-proximal external region of the feline immunodeficiency virus gp36 ectodomain; PA, phosphatidic acid; PC, phosphatidylcholine; PE, phosphatidylethanolamine; PG, phosphatidylglycerol; PS, phosphatidylserine; pre-TM, membrane-proximal segment of the viral glycoprotein; SDS, sodium dodecyl sulfate; TM, transmembrane region of the viral glycoprotein.

10.1021/bi7025062 CCC: $40.75
Published on Web 04/18/2008

cell membrane and competing there with the TM glycoprotein of the virus (*16*). Consequently, an enhancement and strengthening of adhesion to the cell surface is expected to improve antiviral activity of the peptide. From this viewpoint, a suitable strategy is the addition of a lipophilic tail to the peptide molecular structure (*17*). However, such conjugation reactions are never devoid of side effects, because they may result in undesirable structural and chemical changes that could lead to a decrease in biological activity (*18, 19*). In recent work, several of us investigated the antiviral activity of a peptide, named P59, corresponding to the $L^{767}-G^{786}$ sequence (LQKWEDWVGWIGNIPQYLKG) of (TM) gp36 and that of its lipoylated analogue (lipo-P59), which bears a lipophilic tail at the C terminus (*20, 21*). It was found that the two peptides possess similar activity, which, in the case of lipo-P59, is preserved under conditions where the activity of the nonlipoylated peptide was lost. Specifically, when substrate cells were preincubated with the peptides but washed prior to the addition of virus, the lipoylated analogue lipo-P59 retained substantial antiviral activity, whereas that of the nonlipoylated peptide P59 was lost completely. In the same work, the interaction of P59 and lipo-P59 with micellar aggregates formed by dodecylphosphocholine (DPC) and sodium dodecyl sulfate (SDS) was investigated by spectrofluorimetry and circular dichroism (CD). The results showed that both peptides adsorb on the micellar surface, assuming a helical structure. However, no clear evidence for internalization of the lipo-P59 lipophilic chain into the micellar inner core was found in these experiments.

To gain deeper insight into the positioning of P59 and lipo-P59 in lipid membranes, which is crucial for their functionality, a spin-label electron spin resonance (ESR) spectroscopy investigation was undertaken, the results of which are reported in the present work. ESR spectroscopy of spin-labeled lipids is especially well-suited to investigate lipid−protein and lipid−peptide interactions (*22*−*25*). In particular, the site of association (membrane surface or bilayer interior) can be identified unambiguously, and comparison of the results found with different lipids (e.g., charged or uncharged) and under different external conditions (e.g., ionic strength or temperature) gives information on the driving forces, electrostatic versus hydrophobic, of the lipid−peptide interaction. In the present work, the interactions of P59 and lipo-P59 with both zwitterionic and negatively charged lipid bilayer membranes have been investigated using phospholipid ESR probes. In particular, the effects of the lipophilic tail on the mechanism of peptide−membrane binding have been investigated, in order to provide a molecular basis for the results on antiviral activity.

EXPERIMENTAL PROCEDURES

Materials. Dichloromethane and methanol, HPLC-grade solvents, were obtained from Merck (Darmstadt, Germany). The phospholipids, dimyristoyl phosphatidylcholine (DMPC) and dimyristoyl phosphatidylglycerol (DMPG), were obtained from Avanti Polar Lipids (Birmingham, AL). Spin-labeled phosphatidylcholine (1-acyl-2-[*n*-(4,4-dimethyloxazolidinyl-*N*-oxyl)]stearoyl-*sn*-glycero-3-phosphocholine, *n*-PCSL) and phosphatidylglycerol (1-acyl-2-[*n*-(4,4-dimethyloxazolidinyl-*N*-oxyl)]stearoyl-*sn*-glycero-3-phosphoglycerol, *n*-PGSL) with the nitroxide group at different positions, *n*, in the *sn*-2 acyl chain were synthesized as described by Marsh and Watts (*26*). The spin labels were stored at −20 °C in ethanol solutions at a concentration of 1 mg/mL.

Peptide Synthesis. The P59 (LQKWEDWVGWIGNIPQYLKG) peptide and its derivative containing 2-aminooctadecanoic acid (Aod) at the C terminal, lipo-P59 [LQKWEDWVGWIGNIPQYLK(Aod)], were synthesized manually on a solid phase, using standard Fmoc/*t*Bu chemistry, as described elsewhere (*20*). Analytical reverse-phase high-performance liquid chromatography (RP-HPLC) indicated a >97% purity level. The peptides were characterized by mass spectrometry on a Finningan LCQ-Deca ion-trap instrument equipped with an electrospray source (LCQ Deca Finnigan, San Jose, CA); samples were injected directly in the ESI source using a syringe pump at a flow rate of 5 μL/min, and spectral data were analyzed using Xcalibur software.

Sample Preparation. For ESR experiments, appropriate amounts of solutions of DMPC or DMPG in dichloromethane/methanol (2:1, v/v) and spin-label solutions were mixed in small glass tubes. A thin film of the lipid was produced by evaporating the solvent with dry nitrogen gas. Final traces of solvent were removed by subjecting the sample to vacuum desiccation for at least 3 h. The samples were then hydrated with 20−50 μL of 10 mM *N*-(2-hydroxyethyl)piperazine-*N*′-2-ethanesulfonic acid (HEPES), 5 mM ethylenediaminetetraacetic acid (EDTA), and 150 mM NaCl at pH 7.4 buffer (HBS) and vortexed. The lipid suspension thus obtained was transferred to a 100-μL glass capillary and pelleted in a tabletop centrifuge. Excess supernatant was removed, and the capillary was flame-sealed. Samples containing P59 or lipo-P59 were prepared in a similar manner, except that the lipid film was hydrated directly with the peptide solution in buffer (at a concentration of 10 mg/mL). The lipo-P59 solutions are slightly opalescent at room temperature and were gently warmed (40−50 °C) to ensure proper dissolution of the peptide. Samples with P59/DMPC ratios greater than 0.6 wt/wt became optically clear and could no longer be pelleted; therefore, the solubilized sample was used as such for the ESR study. In view of this limitation, the volume of the peptide solution added was minimized by using a higher concentration of P59 (20 mg/mL), such that the amount of sample in the ESR cavity was maximized.

Small-angle neutron scattering revealed that the optically clear samples with P59/DMPC > 0.6 wt/wt consist of rodlike micelles. For a 0.6 wt % dispersion of P59/DMPC (1:1, wt/wt) in HBS at 30 °C, the dependence of the scattering cross-sections on Q-vector is consistent with micellar aggregates of length 350 ± 30 Å and diameter 48 ± 1 Å (see ref *27* for analytical treatment of the data).

ESR Spectroscopy. ESR spectra of lipid and lipid/peptide samples were recorded on a 9-GHz Bruker EMX ESR spectrometer with an ER 041 XK-D microwave bridge. Capillaries containing the samples were placed in a standard 4-mm quartz sample tube containing light silicone oil for thermal stability. The temperature of the sample was regulated and maintained constant during the measurement by blowing thermostatted nitrogen gas through a quartz Dewar. The instrumental settings were as follows: sweep width, 120 G; resolution, 1024 points; modulation frequency, 100 kHz; modulation amplitude, 1.0 G; time constant, 20.5

ms; sweep time, 42 s; incident power, 5.0 mW. Several scans, typically 16, were accumulated to improve the signal-to-noise ratio. Values of the outer hyperfine splitting, $2A_{max}$, were determined by measuring the difference between the low-field maximum and the high-field minimum. Reproducibility in measurement of $2A_{max}$ is typically ±0.1−0.2 G. In general, A_{max} is dependent upon both the amplitude (i.e., order) and rate of chain rotational motion (*28, 29*), and is therefore a useful parameter for characterizing chain dynamics in both gel- and fluid-phase membranes (*30, 31*). It is a sensitive means for detecting and quantifying lipid−protein interactions with peripheral peptides, as demonstrated previously (*32*−*35*). Spectral simulations demonstrate the validity of this approach (*36, 37*).

Fluorescence Measurements. Peptide−liposome interactions were studied by monitoring the changes in the Trp fluorescence emission spectra in the presence of unilamellar vesicles of DMPC. Samples prepared for fluorescence measurements contained peptide (3.5×10^{-5} M) and a 2−20-fold higher concentration (from 7×10^{-5} to 7×10^{-4} M) of phospholipid. Unilamellar vesicles were prepared from multilamellar vesicles by sonication for 3−4 h and repeated extrusion through polycarbonate membranes of 100 nm pore size.

Fluorescence measurements were performed at 30 °C using a Fluorolog-3 spectrofluorimeter (Jobin Yvon). The excitation wavelength was 280 nm, and emission spectra were recorded between 310 and 450 nm, with slit widths of 2 nm.

Thermodynamic Calculations. Free energies of transfer and hydrophobic moments were calculated for the peptides according to the whole-residue scale for transfer from water to the interface, or to octanol, of Wimley and White (*38*). Calculations were made using the Membrane Protein Explorer package (MPEx) of Jayasinghe et al. (*39*). Hydrophobic moments are defined according to ref *40*. Incremental free energies for transfer of methylene groups from water to the hydrocarbon core of the membrane were obtained from the free energies of micellization of lysolipids (*41, 42*).

RESULTS

Peptide Hydropathy. Using the Wimley−White octanol scale (*38*), transfer of P59 from water to the hydrocarbon core of the membrane is predicted to be strongly disfavored energetically. In contrast, transfer of P59 from water to the polar−apolar interface of the membrane is predicted to be energetically favorable. On the Wimley−White interfacial hydropathy scale, the free energy of transfer from water is $\Delta G_{transf} = -4.8$ kJ mol^{-1}, if the N and C termini are charged and the peptide is in a random conformation. This is augmented by an additional −13.3 kJ mol^{-1} if the N and C termini are electroneutral and by a further −1.7 kJ mol^{-1} per residue when helix formation on surface association of the peptide is taken into account (*43*). Thus, the free energy of transfer of P59 from water to the membrane interface is predicted to lie within the range: $\Delta G_{transf} = -4.8$ to −51.6 kJ mol^{-1}, which corresponds to mole-fraction partition coefficients ($K_p = \exp[-\Delta G_{transf}/RT]$) ranging from 7 up to 1.1×10^9. This preferential surface location arises, at least in part, from the strongly amphipathic nature of the peptide in an α-helical conformation, which is predicted to have a hydrophobic moment of $\mu_H = 32.2$ kJ mol^{-1} on the interfacial scale, with the moment directed toward the central tryptophan, W^{773}, of the WX_2WX_2W motif.

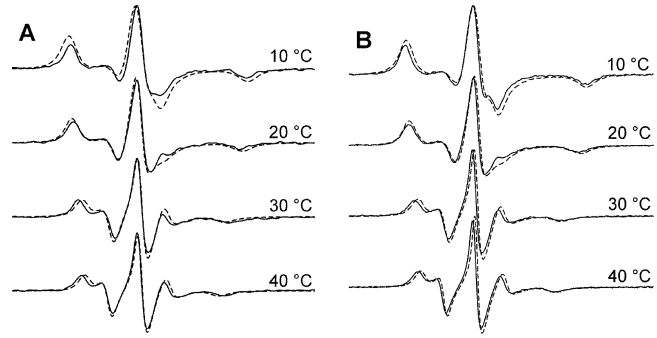

FIGURE 1: ESR spectra of 5-PCSL in dimyristoyl phosphatidylcholine bilayer membranes, in the presence (—) and absence (- - -) of 1:1 (wt/wt) peptide at the temperatures indicated. The plot width is 110 G. (A) P59 and (B) lipo-P59.

The relatively modest partition coefficients at the lower end of the predicted range could explain why activity of P59 is lost in wash-out experiments in cellular systems (*20*). Transfer to the interface of the C-terminal amide that results from linking the lipoyl chain is 8.0 kJ mol^{-1} energetically more favorable than for the ionized C terminus but 3.3 kJ mol^{-1} less favorable than for the protonated C terminus. As will be discussed later, however, burying the hydrocarbon segments of the lipoyl chain entirely in the hydrophobic interior of the membrane is energetically favorable by up to an additional 46.3 kJ mol^{-1}.

Interactions with Phosphatidylcholine and Phosphatidylglycerol Membranes. The association of P59 and lipo-P59 with lipid membranes can be detected from the perturbation of the chain mobility of spin-labeled lipids, using ESR spectroscopy as found for classical water-soluble peripheral membrane proteins (*22, 23, 32, 44*). Because the peptide−lipid interaction can depend upon the state (gel or fluid phase) of the lipid bilayer, we performed a systematic temperature dependence. The samples investigated were phosphatidylcholine spin-labeled on the 5-C atom of the *sn*-2 chain (5-PCSL) incorporated in DMPC membranes, and correspondingly spin-labeled phosphatidylglycerol (5-PGSL) in DMPG membranes, in the presence and in the absence of the peptides P59 or lipo-P59. Selected ESR spectra from the zwitterionic lipid samples are shown in Figure 1; significant perturbations by the peptides are detectable (compare solid and dashed lines). Figure 2 shows the temperature dependences of the outer hyperfine splittings, $2A_{max}$, of 5-PCSL in DMPC membranes and of 5-PGSL in DMPG membranes. For DMPC alone (Figure 2A), a sharp decrease in $2A_{max}$ is evident at ca. 25 °C, corresponding to the increase in lipid chain mobility on the transition from the gel to the fluid phase of the DMPC bilayer (cf. ref *45*). The addition of 1:1 wt/wt peptide (P59 or lipo-P59) with respect to lipid significantly affects the trend in $2A_{max}$ with temperature. Particularly in the fluid membrane phase, $2A_{max}$ is larger in the presence of peptide than in its absence; i.e., the mobility of the spin-labeled chains is decreased by the interaction of the peptide with the membrane. The effect is stronger for P59 than for the lipoylated analogue. Furthermore, the cooperativity of the DMPC chain-melting transition is reduced, while its position remains approximately the same. Also in this respect, the effect of P59 is stronger than that of lipo-P59.

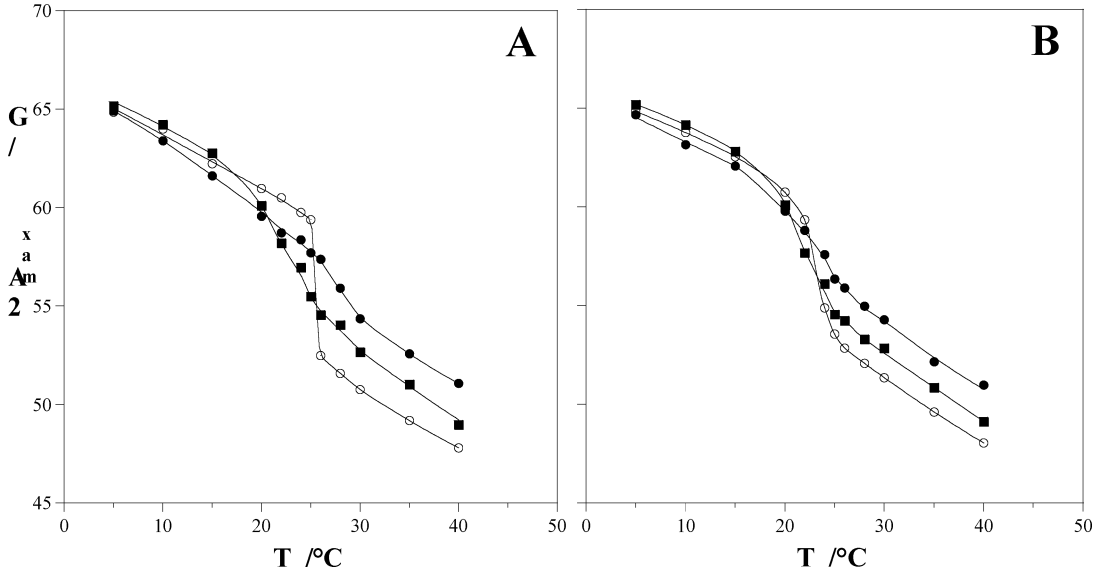

FIGURE 2: Temperature dependence of the outer hyperfine splitting, $2A_{max}$, of 5-position phospholipid spin labels in phospholipid membranes in the absence (○) and presence of 1:1 (wt/wt) P59 (●) or lipo-P59 (■). (A) 5-PCSL in dimyristoyl phosphatidylcholine bilayer membranes and (B) 5-PGSL in dimyristoyl phosphatidylglycerol bilayer membranes.

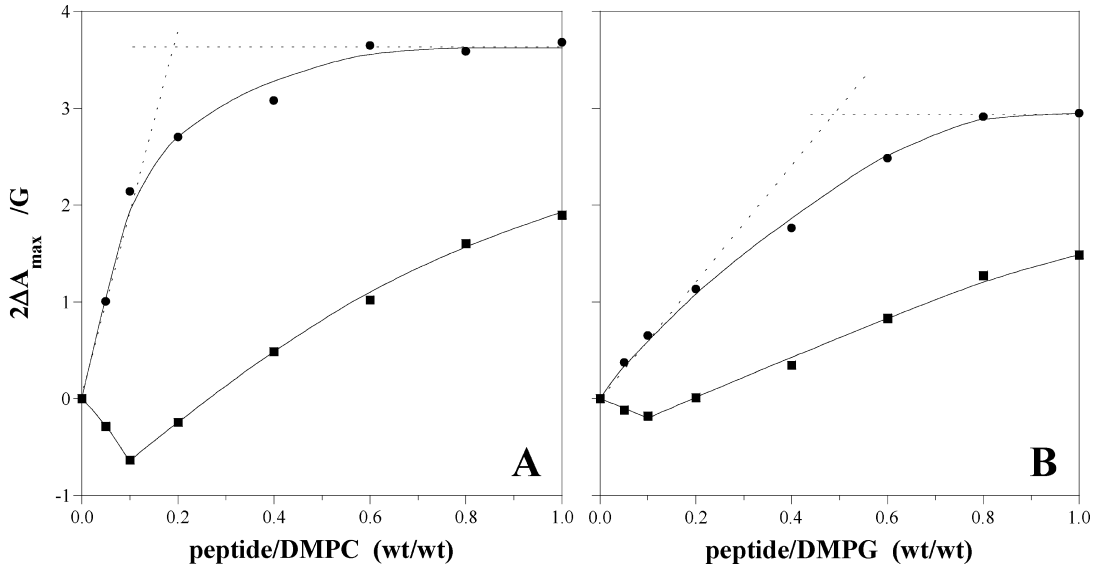

FIGURE 3: Dependence of the increase, $2\Delta A_{max}$, in outer hyperfine splitting of 5-position phospholipid spin labels at 30 °C on the peptide/lipid ratio for P59 (●) or lipo-P59 (■) peptides. (A) 5-PCSL in dimyristoyl phosphatidylcholine bilayer membranes and (B) 5-PGSL in dimyristoyl phosphatidylglycerol bilayer membranes.

Inspection of Figure 2B shows that the behavior of DMPG membranes, in the presence of P59 and lipo-P59, is similar to that of DMPC membranes. The chain-melting transition of the charged lipid (22−24 °C) is less sharp than that of the zwitterionic one and becomes even broader in the presence of the peptides. The values of $2A_{max}$ in the gel phase are less affected by the peptides, while in the fluid phase, a reduction of the spin-label mobility is very evident, particularly in the case of P59.

Peptide−Lipid Titration. Figure 3 shows the increase in outer hyperfine splitting, $2\Delta A_{max}$, of the 5-position spin-labeled lipids in DMPC and DMPG membranes with an increasing peptide concentration. For DMPC membranes in the presence of P59 (see Figure 3A), a typical saturation of binding is registered: the decrease in lipid chain mobility saturates with a value of $2\Delta A_{max} \approx 3.2$ G at a weight ratio of added P59/DMPC of approximately 0.6, which corresponds to ca. 2 lipids per peptide. The stoichiometry of the interaction can be estimated by extrapolation of the increase in $2\Delta A_{max}$, on initial tight binding, to the saturation value of $2\Delta A_{max}$. This gives a value of 1 P59 molecule bound per 15 lipids, which is likely to be an upper estimate because of a possible nonlinear dependence of $2\Delta A_{max}$ on peptide binding. It is important to note that the addition of P59 to multilamellar dispersions of DMPC solubilizes the lipid, so that systems with a peptide/lipid ratio higher than 0.6 (wt/wt) exhibit a transparent appearance. However, the ESR spectra of the spin-labeled lipids are insensitive to this change, showing that the dynamic, liquid-crystalline state of the lipid chains is preserved, despite the change in morphology.

The results found for DMPG membranes in the presence of increasing amounts of P59 are similar to those with DMPC (see Figure 3B), except that saturation is reached at a higher peptide/lipid ratio (0.8 wt/wt) and the initial increase in $2\Delta A_{max}$ is less steep. The stoichiometry of the interaction is estimated to be ca. 4 lipids per peptide, corresponding to

Table 1: Increase in Outer Hyperfine Splitting, $2\Delta A_{max}$, of 5-PCSL Induced by the Interaction of P59 or Lipo-P59 with DMPC Bilayer Membranes, at 30 °C, as a Function of the NaCl Concentration in the Buffer System

	$2\Delta A_{max}$ (G)	
[NaCl] (mM)	DMPC plus P59	DMPC plus lipo-P59
10	3.6	1.9
150	4.3	4.2
500	4.8	5.4

the intersection (at 0.5 wt/wt peptide/lipid ratio) between the initial linear slope and saturation level of the binding curve.

The influence of the lipoylated peptide on the lipid bilayer is very different from that of the nonlipoylated peptide, as shown by the comparison in parts A and B of Figure 3. The interaction of lipo-P59 with both DMPC and DMPG initially causes a slight decrease in $2\Delta A_{max}$, indicating an increase in lipid chain mobility. Above a peptide/lipid ratio of ~0.1 wt/wt, $2\Delta A_{max}$ increases with increasing content of lipoylated peptide, without reaching a clear saturation value in the range of peptide/lipid ratios investigated. The membrane surface charge (i.e., anionic versus zwitterionic lipids) does not change this trend.

Effect of Ionic Strength. The effect of the ionic strength on peptide binding to DMPC membranes was also investigated. Table 1 reports the increase in outer hyperfine splitting, $2\Delta A_{max}$, of 5-PCSL that is induced by the interaction of P59 or lipo-P59 with DMPC bilayer membranes, for buffers containing different concentrations of NaCl. Shielding of electrostatic interactions and possibly modulation of lipid headgroup hydration (cf. ref *46*) increases the binding of both peptides to the bilayers, with the effect being greater for the lipoylated peptide. Indeed, inspection of Table 1 reveals that increasing the ionic strength reduces and almost removes the difference between the effects of P59 and lipo-P59 on lipid chain mobility.

Lipid Chain Flexibility Profiles. Perturbation of the ESR spectra from spin labels at different positions, *n*, in the *sn*-2 chain of the lipid that is induced by binding P59 or lipo-P59 was also investigated. Figure 4 gives the ESR spectra of the *n*-PCSL phosphatidylcholine spin-label positional isomers in fluid DMPC bilayer membranes ($T = 30$ °C), in the presence and absence of the peptide at a peptide/lipid ratio of ~1 wt/wt. In the absence of peptide, the outer hyperfine splitting decreases progressively with increasing *n*, as the spin-label position is stepped down the chain toward

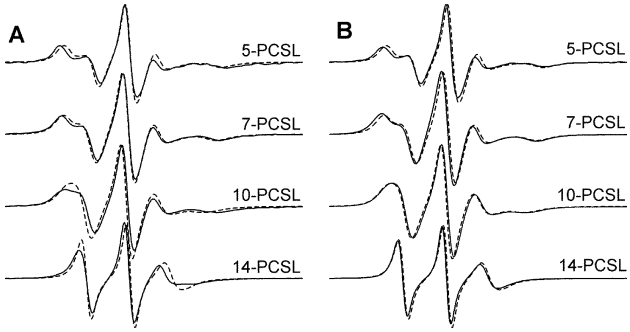

FIGURE 4: ESR spectra of *n*-PCSL positional isomers of spin-labeled phosphatidylcholine in fluid-phase dimyristoyl phosphatidylcholine bilayer membranes, in the presence (—) and absence (- - -) of 1:1 (wt/wt) peptide at 30 °C. Plot width is 110 G. (A) P59 and (B) lipo-P59.

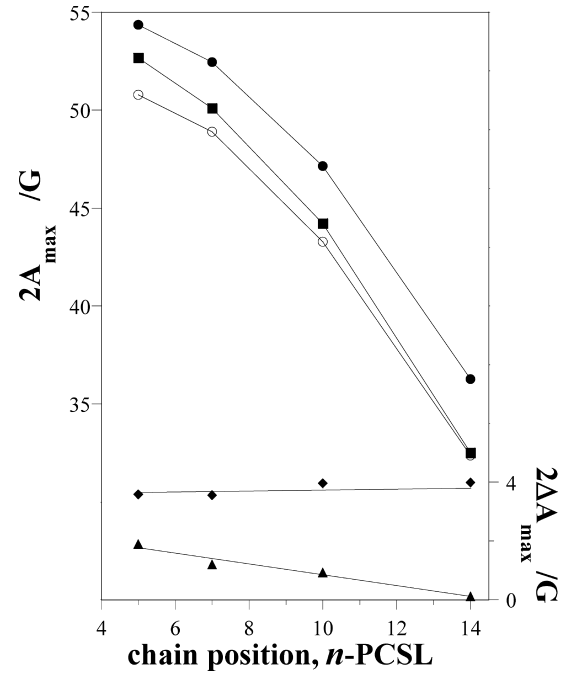

FIGURE 5: Dependence on spin-label position, *n*, of the outer hyperfine splitting, $2A_{max}$ (left-hand ordinate), of the *n*-PCSL phosphatidylcholine spin labels in fluid-phase membranes of DMPC, in the absence (○) and presence of 1:1 (wt/wt) P59 (●) or lipo-P59 (■). $T = 30$ °C. Right-hand ordinate: increase in outer hyperfine splitting, $2\Delta A_{max}$, on adding P59 (◆) or lipo-P59 (▲).

the center of the membrane. As opposed to the clearly defined axially anisotropic spectra that are obtained for 5-PCSL toward the polar headgroup end of the chain, a narrow, three-line, quasi-isotropic spectrum is obtained for 14-PCSL that is positioned close to the terminal methyl region of the chain. This flexibility gradient in segmental chain mobility is a characteristic hallmark of the liquid-crystalline state of fluid phospholipid bilayers (see, e.g., refs *45* and *47*−*49*).

In the presence of bound P59 or lipo-P59, the outer hyperfine splitting is increased at all spin-label chain positions. Figure 5 shows the dependence of the outer hyperfine splitting, $2A_{max}$, on chain position, *n*, for the *n*-PCSL spin labels in fluid DMPC membranes, with and without a saturating amount of peptide. For both peptides, the characteristic flexibility gradient with chain position of the fluid lipid bilayer membranes is preserved. However, inspection of the figure reveals significantly different behavior of the membrane chain mobility in the presence of the two peptides. In fact, P59 causes an increase in $2A_{max}$ to roughly the same extent at all chain positions, whereas the increase in $2A_{max}$ by lipo-P59, which for 5-PCSL is already lower than that caused by P59, decreases further, almost tending to zero, with increasing *n*. This indicates that the increase in lipid packing density, which is induced by surface association of the peptide (cf. refs *32* and *44*), propagates down the chain more effectively in the case of P59 than for the lipoylated peptide, either because of the inherently greater surface perturbation by the former or because of the attenuating and fluidizing effect of the inserted lipoyl chain. For both peptides, there is no appearance of a second, more motionally restricted component in the spectra of the spin labels positioned toward the terminal methyl ends of the chains. This is evidence that the peptides bind solely at the membrane surface and do not penetrate appreciably into the

Table 2: Outer Hyperfine Splittings ($2A_{max}$) of Phospholipid Probes Spin Labeled at the Fifth Position of the *sn*-2 Chain, Incorporated in DMPC Bilayers and Peptide (P59 or Lipo-P59)/DMPC Complexes at 30 °C

	$2A_{max}$ (G)			$2\Delta A_{max}$ (G)	
spin label	DMPC	DMPC plus P59	DMPC plus lipo-P59	DMPC plus P59	DMPC plus lipo-P59
5-PCSL	50.8	54.3	52.7	3.5	1.9
5-PGSL	52.1	53.2	53.2	1.1	1.1
5-PASL	52.3	53.3	52.6	1.0	0.3
5-PESL	52.4	53.3	52.7	0.9	0.3
5-PSSL	53.0	53.9	53.3	0.9	0.3

membrane interior, as does, for instance, the myelin basic protein (*50*−*52*) or apocytochrome *c* (*53*−*55*).

Selectivity of Lipid−*Protein Interaction.* The selectivity of interaction of different lipids with P59 and lipo-P59 bound to DMPC membranes was determined using probe amounts of lipids spin labeled at the 5-C atom of the *sn*-2 chain. Table 2 gives the outer hyperfine splittings ($2A_{max}$) of the spin labels at 30 °C, in the absence and the presence of 1:1 (wt/wt) peptide. For all spin-labeled lipids tested, the outer hyperfine splitting, $2A_{max}$, is greater for the peptide-bound membranes than for the membranes of lipid alone. The increase in $2A_{max}$ differs, however, for the two peptides and for the different spin-labeled lipids. This reflects a selectivity of interaction of both P59 and lipo-P59 with the different lipid polar headgroups. Table 2 gives the increase, $2\Delta A_{max}$, in outer hyperfine splitting for the peptide-bound membranes, relative to that for peptide-free membranes. For both peptides, the largest increase is for 5-PCSL, while the smallest increase is for 5-PESL and 5-PSSL. Furthermore, it is interesting to observe that, for each spin label, $2\Delta A_{max}$ is greater with P59 than with lipo-P59, with the exception of 5-PGSL, which exhibits the same value of $2\Delta A_{max}$ with the two peptides.

Fluorescence Spectra. The fluorescence intensities of some vibronic fine structures in the tryptophan fluorescence spectrum show a strong environmental dependence (*56, 57*). In particular, the emission maximum shifts from 354 to 329 nm when going from water to an apolar medium. The quantum yield can also undergo large changes, the direction and extent of which depend upon the system under consideration (*58*). Fluorescence experiments therefore allow evaluation of the polarity experienced by the tryptophans of P59 and lipo-P59 in DMPC liposomes.

P59 and lipo-P59 in water (parts A and B of Figure 6, respectively) give Trp emission spectra typical of an aqueous environment ($\lambda_{max} \approx 352$ nm), indicating that the tryptophans are exposed to water. For both peptides, the addition of increasing concentrations of DMPC liposomes causes: (i) a shift of the emission maximum to lower wavelengths and (ii) a change in quantum yield. Concerning the first effect, inspection of Figure 6 shows that, whereas in the case of P59, the shift is very weak ($\lambda_{max} = 348$ nm at a 20:1 lipid/peptide molar ratio), that for lipo-P59 is much greater and increases progressively with increasing lipid content, reaching a limiting value of $\lambda_{max} = 339$ nm at a lipid/peptide ratio of 20:1 (mol/mol). Because the Trp emission maximum of P59 does not shift appreciably, the nonlipoylated peptide must remain surface-associated with increasing peptide/lipid ratios and is unlikely to form, e.g., toroidal pores at high peptide/lipid contents.

Interestingly, the changes in quantum yield are in opposite directions for the two peptides; the emission intensity decreases for P59 and increases for lipo-P59. This indicates that the two peptides interact with the bilayer structure through significantly different mechanisms.

DISCUSSION

P59 is a 20-mer peptide (L^{767}−G^{786}) derived from MPER of the FIV gp36 (see Figure 7A); inspection of its sequence shows that it does not contain a preponderance of either acidic or basic residues, being characterized mainly by the presence of three equally spaced tryptophans at positions 770, 773, and 776. CD measurements showed that this peptide, which adopts a predominantly random-coil conformation in water, assumes a turn-helical conformation (see Figure 7B) in the presence of membrane-mimicking systems, such as DPC or SDS micelles (*20*) and dipalmitoyl PC or dipalmitoyl PG liposomes (*21*). High-resolution nuclear magnetic resonance (NMR) analysis in micellar environments revealed that the region endowed with significant structural order along the sequence extends from W^{770} to I^{780} (*21*). In particular, an amphipathic helix forms, in which the polar or charged residues are positioned on one side, as shown in Figure 7B, with the opposite side occupied by hydrophobic residues and by the three tryptophans, which have a propensity to localize to the polar−apolar interface of membranes (*38, 59*). The present results will be discussed in light of these findings and the increased retention of the lipoylated peptide by cellular substrates (*20*).

Perturbation of Chain Mobility. We discuss first the nonlipoylated peptide. P59 decreases the lipid chain motion progressively with increasing peptide/lipid ratio (see Figure 3), and in a manner that is uniform throughout the bilayer membrane (see Figure 5). This is consistent with a purely surface association (*31*−*33, 44*), without deep penetration, as suggested also by the small red shift and low quantum yield of tryptophan fluorescence (see Figure 6A). A further possibility is the formation of toroidal pores (cf. ref *60*), in which the peptide effectively still maintains a surface association. As already pointed out, however, the near constancy in position of the tryptophan emission maximum of P59 with peptide/lipid ratio suggests a constant surface association without induction of toroidal pores at higher peptide contents.

Figure 8 collects together ESR data from different proteins and peptides that are bound to DMPG membranes and compares these with the present data from P59 (and lipo-P59). The perturbation by P59 is among the smallest. Significantly, it is comparable to that by truncated α-synuclein, which consists of the N-terminal section bearing the 11-residue repeats that are homologous to the amphipathic helices in the lipid-binding domains of exchangeable serum apolipoproteins (*34*).

Unlike most of the basic proteins shown in Figure 8, P59 perturbs the chain mobility of zwitterionic DMPC to a comparable extent to anionic DMPG bilayers (see Figure 2). This can be attributed to the amphipathic nature of the peptide and the interfacially localizing tryptophan residues that recur at positions i and $i + 3$. The increase in outer hyperfine splitting of 5-PCSL that is induced by binding P59 to DMPC is $2\Delta A_{max} = 3.6$ G (see Table 1). For comparison, that induced in DMPC by membrane-penetrating α-lactalbumin at low pH is $2\Delta A_{max} = 2.6$ G at 30 °C (*61*); and that

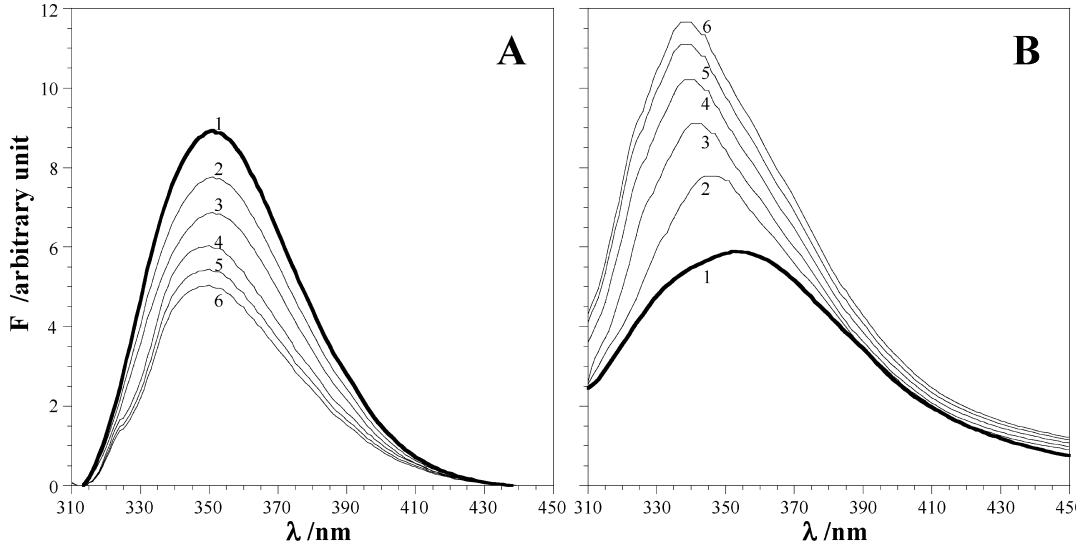

FIGURE 6: Tryptophan emission spectra (range 310−450 nm) of P59 (A) and lipo-P59 (B) in aqueous phosphate buffer (1, heavy line) and in the presence of DMPC small unilamellar liposomes at increasing lipid/peptide molar ratios: 2, 2:1; 3, 4:1; 4, 7:1; 5, 10:1; and 6, 20:1 (light lines).

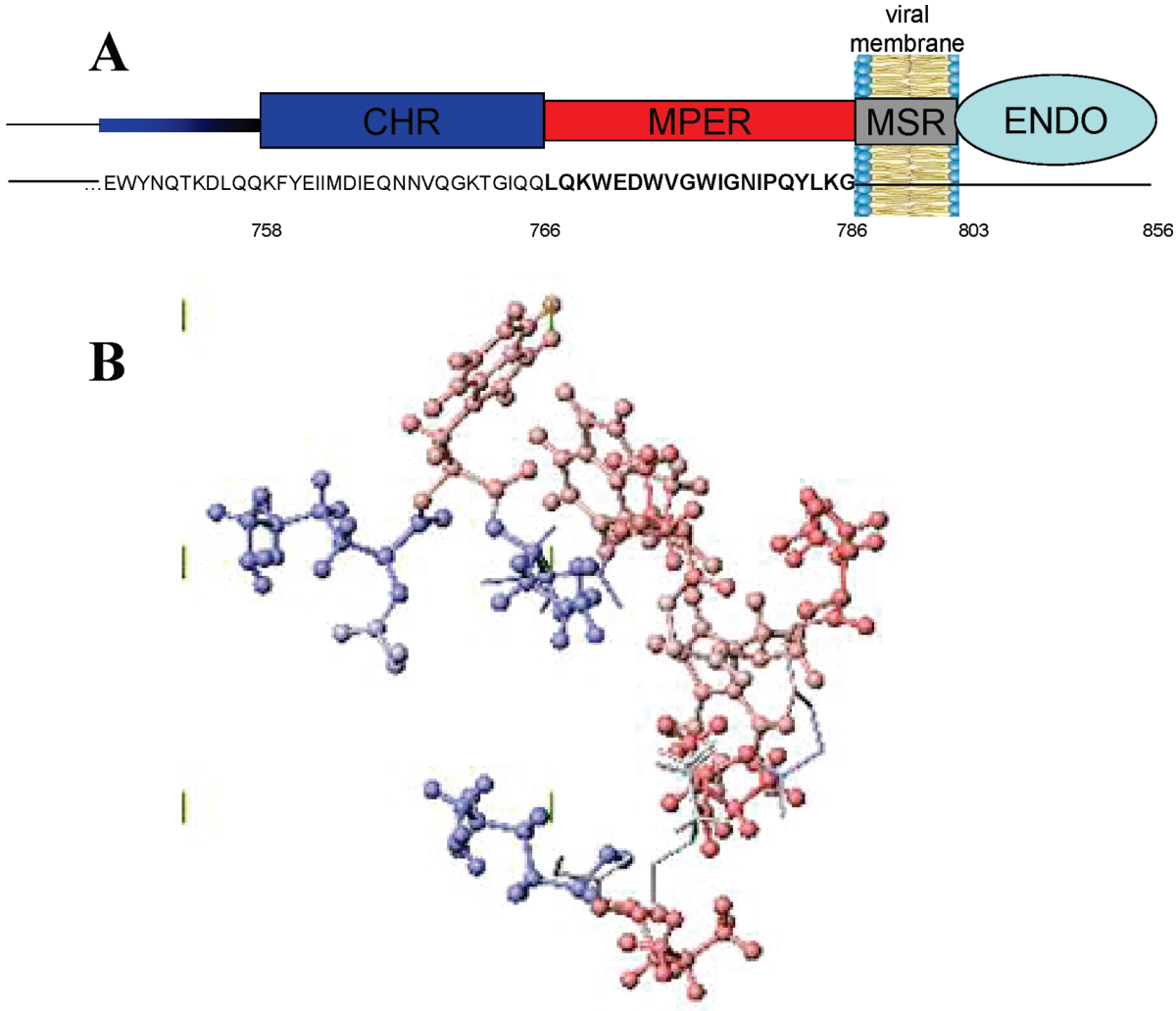

FIGURE 7: (A) Schematic representation of the C-terminal region of gp36; the P59 sequence is highlighted in bold. Domains are indicated as follows: CHR, C-terminal α-helix region; MPER, membrane-proximal external region; MSR, membrane-spanning region; and ENDO, interior region. (B) P59 structure in a micellar environment, as derived from high-resolution NMR analysis (*21*). The polar and apolar residues are in blue and red, respectively. Vertical bars indicate the positions of the three tryptophan residues.

for nonpenetrating peptides is $2\Delta A_{max} = 0.7$, 0.4, and close to 0 G, for truncated α-synuclein (*34*), melittin (*31*), and full-length α-synuclein (*32*), respectively. Absorption of human serum albumin to dipalmitoyl PC decreases the outer hyperfine splitting by $2\Delta A_{max} \approx 0.2-0.4$ G for 5-PCSL in the fluid phase (*62*). Thus, the perturbation induced by

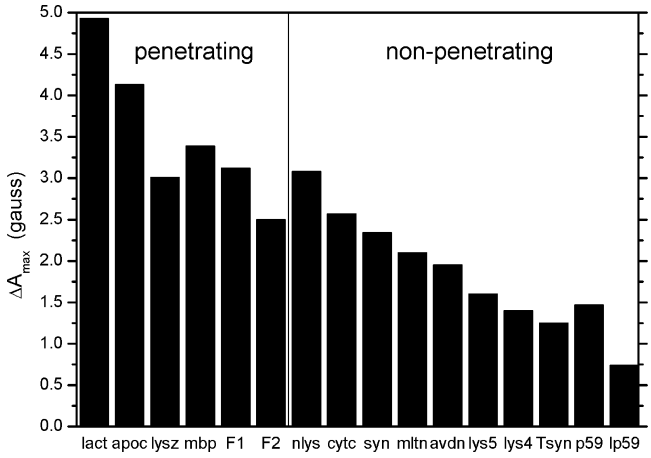

FIGURE 8: Increase in outer hyperfine splitting of 5-PGSL in DMPG membranes on adding saturating amounts of surface-associating proteins or peptides. $T = 30$ °C. Buffers contain 10 mM NaCl. Peptides that partially penetrate the lipid bilayer are (from left to right) α-lactalbumin at pH 4 [lact (*61*)], apocytochrome *c* [apoc (*53*)], lysozyme [lysz (*35*)], myelin basic protein [mbp (*52*)], and complementary fragments of mbp [F1 and F2 (*51*)]. Peptides that do not penetrate the lipid bilayer are (from left to right) polysine [nlys (*35*)], cytochrome *c* [cytc (*35*)], α-synuclein [syn (*32*)], mellitin [mltn (*31*)], avidin [avdn (*44*)], pentalysine and tetralysine [lys5 and lys4 (*33*)], truncated α-synuclein [Tsyn (*34*)], and P59 and lipo-P59 (p59 and lp59).

binding P59 to zwitterionic lipids is among the larger of those induced by nonpenetrating peptides or proteins. Most likely this is attributable to the interfacial anchoring propensity of the special WX_2WX_2W motif (cf. ref *38*).

Attachment of the lipid chain to P59 has the effect of reducing the net perturbation of the bilayer chain mobility by the peptide (see Figure 2). From the protein/lipid titration in Figure 3, it is seen that $2\Delta A_{max}$ initially decreases with increasing lipo-P59/lipid ratio, quite unlike the situation with the nonlipoylated P59. This increase in mobility is presumably a consequence of inserting the lipoyl chain into the bilayer membrane. The biphasic response to lipo-P59/lipid ratio in Figure 3, therefore represents a competition between this fluidizing tendency of the lipoyl tail and the immobilizing tendency from surface association of the peptide portion of lipo-P59, which is the only effect that is observed for P59 without the lipoyl chain. Under these circumstances, the net change in $2\Delta A_{max}$ by lipo-P59 cannot be compared to values for purely surface-associating, nonlipoylated peptides and proteins in Figure 8. All that can be said is that the effective value for comparison with surface-associated peptides must be larger than the net value of $2\Delta A_{max}$ that is measured.

Insertion of the lipoyl tail suggests that lipo-P59 is anchored more strongly and possibly penetrates more deeply into the membrane than does P59. Indeed, the fluorescence results suggest that the tryptophan residues of lipo-P59 penetrate the membrane more deeply than do those of P59, because the spectral red shift is much larger and the quantum yield is much greater for the former (see Figure 6). This insertion of the lipo-P59 chain, coupled with closer interfacial association of the tryptophans, might stabilize the bilayer, with the result that the bilayer is not fragmented into micelles at high peptide/lipid ratios as is observed for nonlipoylated P59.

Insertion of the lipoyl chain into the membrane could also explain the retention of lipo-P59 activity in wash-out experiments, where the activity of P59 is completely lost (*20*). Transfer of hydrocarbon chains from water to the bilayer interior is energetically favorable by ~2.7 kJ mol^{-1} per CH_2 (*41, 42*), which corresponds to an increase in the binding constant of lipo-P59 by 10^8-fold, relative to P59 without the C18 chain. This effect is sufficiently large to explain the retention of lipo-P59 by membranes, even if the chain is not completely inserted into the hydrophobic interior of the membrane.

Peptide−Lipid Stoichiometry. The peptide−lipid titrations indicate that the stoichiometries at maximum binding correspond to ca. 15 lipids per P59 bound to DMPC and ca. 4 lipids per P59 bound to DMPG (see Figure 3). For tightly packed α-helices of diameter 1.0 nm and 20 residues in length, complete surface coverage would correspond to ca. 5 fluid lipids of cross-sectional area 0.6 nm^2 (cf. ref *63*). An effective diameter of 1.0 nm corresponds to the center−center distance of α-helices that are packed in helix bundles (see, e.g., ref *64*). Thus, for saturation binding to DMPG, the P59 peptides must be tightly packed on the membrane surface. For the structure shown in Figure 7, the area projected onto the membrane surface is 4.7 nm^2, when the three tryptophan residues are located at the polar−apolar interface. This projected area of the bound peptide would cover approximately 8 lipids, which is still less than the binding stoichiometry of P59 with DMPC. At saturation binding to DMPC, the P59 peptides must be packed less tightly than with DMPG and, most likely, are two-dimensionally disordered on the membrane.

Unfortunately, the biphasic nature of the protein−lipid titration curves for the lipoylated peptide does not allow for direct estimation of the stoichiometry at saturation binding. However, the trends in Figure 3 suggest that the numbers of lipids per bound lipo-P59 are less than for the nonlipoylated P59. Insertion of the lipoyl chain into the bilayer will tend to increase the surface area of the membrane. This will allow accommodation of more peptides at the membrane surface and decrease the apparent phospholipid stoichiometry by approximately 0.5 per peptide, possibly by more, in view of the initial decrease in ΔA_{max} on adding lipo-P59 (see Figure 3). Any mechanism that increases the amount of membrane-bound peptide will tend to increase the antiviral efficacy of the peptides. This includes the presence of negatively charged lipids and addition of the lipoyl chain.

Lipid Selectivity. With certain assumptions, including those of fast lipid exchange on the spin-label ESR time scale, the increase in outer hyperfine splitting, ΔA_{max}, for different 5-position spin-labeled lipid species can be related to their relative association constants with the protein (*32, 35*). The selectivity pattern for interaction with P59 in DMPC is therefore in the order: PC > PG ≈ PA ≈ PE ≈ PS, and that for lipo-P59 is PC > PG > PA ≈ PE ≈ PS (see Table 2). For comparison, the lipid spin-label selectivity ranking for melittin bound to DMPC is PG ≈ PE > PS ≫ PC (*31*). The unique predominance of PC interactions for P59 and lipo-59 presumably is attributable to the special interfacially locating WX_2WX_2W motif, and the lack of a net charge and of localized charge clusters.

Ionic Strength Dependence. The P59 peptide contains two basic and two acidic residues but no net charge. The zwitterionic phosphatidylcholine lipids of the bilayer membrane also bear no net charge. Nevertheless, the results of Table 1 are consistent with screening a net repulsive

electrostatic interaction when the NaCl concentration is increased from 10 to 150 mM. A further increase in the NaCl concentration to 500 mM produces a considerably smaller effect, as expected for classical ionic screening. Experiments with anionic lipid bilayers indicate that electrostatic effects are fully screened in 1 M NaCl and that increasing the NaCl concentration beyond this reduces the strength of the polar headgroup hydration (*46, 65, 66*). It is therefore possible that the effects of increasing the salt concentration that are observed here involve both local electrostatics and the effects on hydration of polar groups in both lipid and protein.

Whatever the mechanism, it is clear that neither local electrostatics nor hydration are responsible for the binding of P59 or lipo-P59 to phosphatidylcholine, because increasing the NaCl concentration, which screens electrostatics and weakens hydration, increases the strength of binding. In addition, effects with anionic DMPG are similar to those with zwitterionic DMPC (see Figure 2), which indicates that simple electrostatics are unimportant and consistent with the zero net charge of P59.

CONCLUSIONS

ESR experiments using spin-labeled lipids demonstrate, consistent with thermodynamic predictions, that the P59 and lipo-P59 peptides associate with lipid bilayers by binding at the membrane surface or polar−apolar interface. Additionally, the lipoyl chain of lipo-P59 inserts between those of the lipid bilayer. This stabilizes the bilayer against the surface-active, solubilizing tendency of P59 without the chain, anchors the peptide more strongly to the membrane, thus enhancing long-term antiviral activity, and may also increase the capacity to bind to the membrane.

The mechanism of binding P59 to phospholipid membranes is primarily amphipathic, i.e., driven by interfacial hydrophobic interactions, and not electrostatic. This is seen by comparison of results from DMPC membranes with those from DMPG membranes and from the dependence on the ionic strength. Previous experiments with SDS micelles suggested the importance of attractive electrostatic interactions. This is certainly not the case with anionic phospholipid membranes, such as DMPG. A similar discrepancy has been reported recently for other peptides interacting with plasma membranes (*67*), and points to the limitations of using micelles as membrane-mimicking systems.

The present results may also shed light on the role played by the MPER domain of the FIV or HIV surface glycoprotein in fusion of the viral and target-cell phospholipid membranes. Particularly, the destabilizing effect exerted by the P59 sequence on the membranes, which is highlighted in the present work, could be fundamental to the fusion process. Indeed, the presence of the MPER domain has been shown to be crucial in the infection pathway (*68*). In gp36, the MPER domain is located very close to the viral membrane, but definitely protruding from it. From this viewpoint, its positioning could be similar to that found here for the peptidic sequence of lipo-P59. Consequently, in this starting configuration, it is not expected to exert its destabilizing action on the viral membrane. However, once the fusion peptide has entered the target-cell membrane and subsequent conformational changes in the glycoprotein have brought the two membranes into close proximity, the MPER domain could then destabilize the bilayer of the target cell, thus promoting membrane fusion.

ACKNOWLEDGMENT

We thank Gaetano Mangiapia for carrying out the SANS measurement and Brigitta Angerstein for synthesis of spin-labeled lipids.

REFERENCES

1. Earp, L. J., Delos, S. E., Park, H. E., and White, J. M. (2005) The many mechanisms of viral membrane fusion proteins. *Curr. Top. Microbiol. Immunol. 285*, 25–66.
2. Pedersen, N. C., Ho, E. W., Brown, M. L., and Yamamoto, J. K. (1987) Isolation of a T-lymphotropic virus from domestic cats with an immunodeficiency-like syndrome. *Science 235*, 790–793.
3. Lee, T., Laco, G. S., Torbett, B. E., Fox, H. S., Lerner, D. L., Elder, J. H., and Wong, C. H. (1998) Analysis of the S3 and S3′ subsite specificities of feline immunodeficiency virus (FIV) protease: Development of a broad-based protease inhibitor efficacious against FIV, SIV, and HIV *in vitro* and *ex vivo*. *Proc. Natl. Acad. Sci. U.S.A. 95*, 939–944.
4. Pancino, G., Camoin, L., and Sonigo, P. (1995) Structural analysis of the principal immunodominant domain of the feline immunodeficiency virus transmembrane glycoprotein. *J. Virol. 69*, 2110–2118.
5. Serres, P. F. (2000) Molecular mimicry between the trimeric ectodomain of the transmembrane protein of immunosuppressive lentiviruses (HIV−SIV−FIV) and interleukin 2. *C. R. Acad. Sci., Ser. III 323*, 1019–1029.
6. Frey, S. C., Hoover, E. A., and Mullins, J. I. (2001) Feline immunodeficiency virus cell entry. *J. Virol. 75*, 5433–5440.
7. Giannecchini, S., Bonci, F., Pistello, M., Matteucci, D., Sichi, O., Rovero, P., and Bendinelli, M. (2004) The membrane-proximal tryptophan-rich region in the transmembrane glycoprotein ectodomain of feline immunodeficiency virus is important for cell entry. *Virology 320*, 156–166.
8. Suarez, T., Nir, S., Goñi, F. M., Saez-Cirion, A., and Nieva, J. L. (2000) The pre-transmembrane region of the human immunodeficiency virus type-1 glycoprotein: A novel fusogenic sequence. *FEBS Lett. 477*, 145–149.
9. Salzwedel, K., West, J. T., and Hunter, E. (1999) A conserved tryptophan-rich motif in the membrane-proximal region of the human immunodeficiency virus type 1 gp41 ectodomain is important for Env-mediated fusion and virus infectivity. *J. Virol. 73*, 2469–2480.
10. Jiang, S., Lin, K., Strick, N., and Neurath, A. R. (1993) HIV-1 inhibition by a peptide. *Nature 365*, 113.
11. Jin, B., Jin, S., Ryu, R., Ahn, K., and Yu, Y. G. (2000) Design of a peptide inhibitor that blocks the cell fusion mediated by glycoprotein 41 of human immunodeficiency virus type 1. *AIDS Res. Hum. Retroviruses 16*, 1797–1804.
12. Wild, C. T., Shugars, D. C., Greenwell, T. K., McDanal, C. B., and Matthews, T. J. (1994) Peptides corresponding to a predictive α-helical domain of human immunodeficiency virus type 1 gp41 are potent inhibitors of virus infection. *Proc. Natl. Acad. Sci. U.S.A. 91*, 9770–9774.
13. Kilby, J. M., Lalezari, J. P., Eron, J. J., Carlson, M., Cohen, C., Arduino, R. C., Goodgame, J. C., Gallant, J. E., Volberding, P., Murphy, R. L., Valentine, F., Saag, M. S., Nelson, E. L., Sista, P. R., and Dusek, A. (2002) The safety, plasma pharmacokinetics, and antiviral activity of subcutaneous enfuvirtide (T-20), a peptide inhibitor of gp41-mediated virus fusion, in HIV-infected adults. *AIDS Res. Hum. Retroviruses 18*, 685–693.
14. Massi, C., Indino, E., Lami, C., Fissi, A., Pieroni, O., La Rosa, C., Esposito, F., Galoppini, C., Rovero, P., Bandecchi, P., Bendinelli, M., and Garzelli, C. (1998) The antiviral activity of a synthetic peptide derived from the envelope SU glycoprotein of feline immunodeficiency virus maps in correspondence of an amphipathic helical segment. *Biochem. Biophys. Res. Commun. 246*, 160–165.
15. Giannecchini, S., Di Fenza, A., D'Ursi, A. M., Matteucci, D., Rovero, P., and Bendinelli, M. (2003) Antiviral activity and conformational features of an octapeptide derived from the membrane-proximal ectodomain of the feline immunodeficiency virus transmembrane glycoprotein. *J. Virol. 77*, 3724–3733.

16. Schibli, D. J., Montelaro, R. C., and Vogel, H. J. (2001) The membrane-proximal tryptophan-rich region of the HIV glycoprotein, gp41, forms a well-defined helix in dodecylphosphocholine micelles. *Biochemistry 40*, 9570–9578.
17. Epand, R. M. (1997) Biophysical studies of lipopeptide−membrane interactions. *Biopolymers 43*, 15–24.
18. Ng, K., Zhao, L., Meyer, J. D., Rittman-Grauer, L., and Manning, M. C. (1997) Use of circular dichroism spectroscopy in determining the conformation of a monoclonal antibody prior to its incorporation in an immunoliposome. *J. Pharm. Biomed. Anal. 16*, 507–513.
19. Romano, R., Musiol, H. J., Weyher, E., Dufresne, M., and Moroder, L. (1992) Peptide hormone−membrane interactions: The aggregational and conformational state of lipo-gastrin derivatives and their receptor binding affinity. *Biopolymers 32*, 1545–1558.
20. Esposito, C., D'Errico, G., Armenante, M. R., Giannecchini, S., Bendinelli, M., Rovero, P., and D'Ursi, A. M. (2006) Physicochemical characterization of a peptide deriving from the glycoprotein gp36 of the feline immunodeficiency virus and its lipoylated analogue in micellar systems. *Biochim. Biophys. Acta 1758*, 1653–1661.
21. Giannecchini, S., D'Ursi, A. M., Esposito, C., Scrima, M., Zabogli, E., Freer, G., Rovero, P., and Bendinelli, M. (2007) Antibodies generated in cats by a lipopeptide reproducing the membrane-proximal external region of the feline immunodeficiency virus transmembrane enhance virus infectivity. *Clin. Vaccine Immunol. 14*, 944–951.
22. Marsh, D., and Horváth, L. I. (1998) Structure, dynamics and composition of the lipid−protein interface. Perspectives from spin-labelling. *Biochim. Biophys. Acta 1376*, 267–296.
23. Sankaram, M. B., and Marsh, D. (1993) Protein−lipid interactions with peripheral membrane proteins, in *New Comprehensive Biochemistry: Protein−Lipid Interactions*, Vol. 25, pp 127−162 (Watts, A., Ed.) Elsevier, Amsterdam, The Netherlands.
24. Marsh, D., and Páli, T. (2004) The protein−lipid interface: Perspectives from magnetic resonance and crystal structures. *Biochim. Biophys. Acta 1666*, 118–141.
25. Marsh, D. (2008) Protein modulation of lipids and vice versa in membranes, *Biochim. Biophys. Acta*, in press, doi: 10.1016/j.bbamem.2008.01.015.
26. Marsh, D., and Watts, A. (1982) Spin-labeling and lipid−protein interactions in membranes, in *Lipid−Protein Interactions*, Vol. 2, pp 53−126 (Jost, P. C., and Griffith, O. H., Eds.) Wiley-Interscience, New York.
27. Vaccaro, M., Accardo, A., Tesauro, D., Mangiapia, G., Löf, D., Schillén, K., Söderman, O., Morelli, G., and Paduano, L. (2006) Supramolecular aggregates of amphiphilic gadolinium complexes as blood pool MRI/MRA contrast agents: Physicochemical characterization. *Langmuir 22*, 6635–6643.
28. Lange, A., Marsh, D., Wassmer, K.-H., Meier, P., and Kothe, G. (1985) Electron spin resonance study of phospholipid membranes employing a comprehensive line-shape model. *Biochemistry 24*, 4383–4392.
29. Moser, M., Marsh, D., Meier, P., Wassmer, K.-H., and Kothe, G. (1989) Chain configuration and flexibility gradient in phospholipid membranes. Comparison between spin-label electron spin resonance and deuteron nuclear magnetic resonance, and identification of new conformations. *Biophys. J. 55*, 111–123.
30. Rama Krishna, Y. V. S., and Marsh, D. (1990) Spin label ESR and ^{31}P-NMR studies of the cubic and inverted hexagonal phases of dimyristoylphosphatidylcholine/myristic acid (1:2, mol/mol) mixtures. *Biochim. Biophys. Acta 1024*, 89–94.
31. Kleinschmidt, J. H., Mahaney, J. E., Thomas, D. D., and Marsh, D. (1997) Interaction of bee venom melittin with zwitterionic and negatively charged phospholipid bilayers: A spin-label electron spin resonance study. *Biophys. J. 72*, 767–778.
32. Ramakrishnan, M., Jensen, P. H., and Marsh, D. (2003) α-Synuclein association with phosphatidylglycerol probed by lipid spin labels. *Biochemistry 42*, 12919–12926.
33. Kleinschmidt, J. H., and Marsh, D. (1997) Spin-label electron spin resonance studies on the interactions of lysine peptides with phospholipid membranes. *Biophys. J. 73*, 2546–2555.
34. Ramakrishnan, M., Jensen, P. H., and Marsh, D. (2006) Association of α-synuclein and mutants with lipid membranes: Spin-label ESR and polarized IR. *Biochemistry 45*, 3386–3395.
35. Sankaram, M. B., De Kruijff, B., and Marsh, D. (1989) Selectivity of interaction of spin-labelled lipids with peripheral proteins bound to dimyristoylphosphatidylglycerol bilayers, as determined by ESR spectroscopy. *Biochim. Biophys. Acta 986*, 315–320.
36. Schorn, K., and Marsh, D. (1997) Extracting order parameters from powder EPR lineshapes for spin-labelled lipids in membranes. *Spectrochim. Acta, Part A 53*, 2235–2240.
37. Schorn, K., and Marsh, D. (1996) Lipid chain dynamics in diacylglycerol−phosphatidylcholine mixtures studied by slow-motional simulations of spin label ESR spectra. *Chem. Phys. Lipids 82*, 7–14.
38. White, S. H., and Wimley, W. C. (1998) Hydrophobic interactions of peptides with membrane interfaces. *Biochim. Biophys. Acta 1376*, 339–352.
39. Jayasinghe, S., Hristova, K., and White, S. H. (2001) Energetics, stability, and prediction of transmembrane helices. *J. Mol. Biol. 312*, 927–934.
40. Eisenberg, D., Schwarz, E., Komaromy, M., and Wall, R. (1984) Analysis of membrane and surface protein sequences with the hydrophobic moment plot. *J. Mol. Biol. 179*, 125–142.
41. King, M. D., and Marsh, D. (1987) Headgroup and chain length dependence of phospholipid self-assembly studied by spin-label electron spin resonance. *Biochemistry 26*, 1224–1231.
42. King, M. D., and Marsh, D. (1986) Prediction of the critical micelle concentrations of mono- and di-acyl phospholipids. *Chem. Phys. Lipids 42*, 271–277.
43. Ladokhin, A. S., and White, S. H. (1999) Folding of amphipathic α-helices on membranes: Energetics of helix formation by melittin. *J. Mol. Biol. 285*, 1363–1369.
44. Swamy, M. J., and Marsh, D. (2001) Spin-label electron paramagnetic resonance studies on the interaction of avidin with dimyristoyl−phosphatidylglycerol membranes. *Biochim. Biophys. Acta 1513*, 122–130.
45. Swamy, M. J., and Marsh, D. (1994) Spin-label electron spin resonance studies on the dynamics of the different phases of *N*-biotinylphosphatidylethanolamines. *Biochemistry 33*, 11656–11663.
46. Cevc, G., Watts, A., and Marsh, D. (1981) Titration of the phase transition of phosphatidylserine bilayer membranes. Effects of pH, surface electrostatics, ion binding and headgroup hydration. *Biochemistry 20*, 4955–4965.
47. Bartucci, R., Páli, T., and Marsh, D. (1993) Lipid chain motion in an interdigitated gel phase: Conventional and saturation transfer ESR of spin-labelled lipids in dipalmitoylphosphatidylcholine−glycerol dispersions. *Biochemistry 32*, 274–281.
48. Pates, R. D., and Marsh, D. (1987) Lipid mobility and order in bovine rod outer segment disk membranes. A spin-label study of lipid−protein interactions. *Biochemistry 26*, 29–39.
49. Fretten, P., Morris, S. J., Watts, A., and Marsh, D. (1980) Lipid−lipid and lipid−protein interactions in chromaffin granule membranes. *Biochim. Biophys. Acta 598*, 247–259.
50. Sankaram, M. B., Brophy, P. J., and Marsh, D. (1989) Spin label ESR studies on the interaction of bovine spinal cord myelin basic protein with dimyristoylphosphatidylglycerol dispersions. *Biochemistry 28*, 9685–9691.
51. Sankaram, M. B., Brophy, P. J., and Marsh, D. (1989) Interaction of two complementary fragments of the bovine spinal cord myelin basic protein with phospholipid bilayers. An ESR spin label study. *Biochemistry 28*, 9692–9698.
52. Sankaram, M. B., Brophy, P. J., and Marsh, D. (1989) Selectivity of interaction of phospholipids with bovine spinal cord myelin basic protein studied by spin-label electron spin resonance. *Biochemistry 28*, 9699–9707.
53. Görrissen, H., Marsh, D., Rietveld, A., and De Kruijff, B. (1986) Apocytochrome *c* binding to negatively charged lipid dispersions studied by spin-label electron spin resonance. *Biochemistry 25*, 2904–2910.
54. Rietveld, A., Ponjee, G. A. E., Schiffers, P., Jordi, W., van de Coolwijk, P. J. F. M., Demel, R. A., Marsh, D., and De Kruijff, B. (1985) Investigations on the insertion of the mitochondrial precursor protein apocytochrome *c* into model membranes. *Biochim. Biophys. Acta 818*, 398–409.
55. Rietveld, A., Berkhout, T. A., Roenhorst, A., Marsh, D., and De Kruijff, B. (1986) Preferential association of apocytochrome *c* with negatively charged phospholipids in mixed model membranes. *Biochim. Biophys. Acta 858*, 38–46.
56. Konev, S. V. (1967) *Fluorescence and Phosphorescence of Proteins and Nucleic Acids*, Plenum Press, New York.
57. Ambrosone, L., D'Errico, G., and Ragone, R. (1997) Interaction of tryptophan and *N*-acetyltryptophanamide with dodecylpentaoxyethyleneglycol ether micelles. *Spectrochim. Acta 53*, 1615–1620.

58. Callis, P. R., and Liu, T. Q. (2004) Quantitative prediction of fluorescence quantum yields for tryptophan in proteins. *J. Phys. Chem. B 108*, 4248–4259.
59. de Planque, M. R. R., Greathouse, D. V., Koeppe, R. E., II, Schäfer, H., Marsh, D., and Killian, J. A. (1998) Influence of lipid/peptide hydrophobic mismatch on the thickness of diacylphosphatidylcholine bilayers. A ^{2}H NMR and ESR study using designed transmembrane α-helical peptides and gramicidin A. *Biochemistry 37*, 9333–9345.
60. Pistolesi, S., Pogni, R., and Feix, J. B. (2007) Membrane insertion and bilayer perturbation by antimicrobial peptide CM15. *Biophys. J. 93*, 1651–1660.
61. Montich, G. G., and Marsh, D. (1995) Interaction of α-lactalbumin with phosphatidylglycerol. Influence of protein binding on the lipid phase transition and lipid acyl chain mobility. *Biochemistry 34*, 13139–13145.
62. Bartucci, R., Pantusa, M., Marsh, D., and Sportelli, L. (2002) Interaction of human serum albumin with membranes containing polymer-grafted lipids: Spin-label ESR studies in the mushroom and brush regimes. *Biochim. Biophys. Acta 1564*, 237–242.
63. Marsh, D. (1990) *Handbook of Lipid Bilayers*, CRC Press, Boca Raton, FL.
64. Marsh, D. (1997) Stoichiometry of lipid−protein interaction and integral membrane protein structure. *Eur. Biophys. J. 26*, 203–208.
65. Cevc, G., Watts, A., and Marsh, D. (1980) Non-electrostatic contribution to the titration of the ordered-fluid phase transition of phosphatidylglycerol bilayers. *FEBS Lett. 120*, 267–270.
66. Cevc, G., Seddon, J. M., and Marsh, D. (1985) Thermodynamic and structural properties of phosphatidylserine bilayer membranes in the presence of lithium ions and protons. *Biochim. Biophys. Acta 814*, 141–150.
67. Esposito, C., Scrima, M., Carotenuto, A., Tedeschi, A. M., Rovero, P., and D'Errico, G. (2007) Structures and micelle locations of the non lipidated and lipidated C-terminal membrane anchor of 2′,3′-cyclic nucleotide-3′-phosphodiesterase. *Biochemistry 47*, 308–319.
68. Barbato, G., Bianchi, E., Ingallinella, P., Hurni, W. H., Miller, M. D., Ciliberto, G., Cortese, R., Bazzo, R., Shiver, J. W., and Pessi, A. (2003) Structural analysis of the epitope of the anti-HIV antibody 2F5 sheds light into its mechanism of neutralization and HIV fusion. *J. Mol. Biol. 330*, 1101–1115.

BI7025062